Supplementary material for: Compressibility of synthetic Mg-Al tourmalines to 60 GPa

Eleanor J. Berryman[1], Dongzhou Zhang[2], Bernd Wunder[3], Thomas S. Duffy[1]

[1]Department of Geosciences, Princeton University, Princeton, NJ 08544, USA
[2]Hawai'i Institute of Geophysics and Planetology, University of Hawai'i at Monoa, Honolulu, HI 96822, USA
[3]Chemistry and Physics of Earth Materials, GFZ German Research Centre for Geosciences, 14473 Potsdam, Germany

The following supplementary information is provided here:

1. Dravite and K-dravite synthesis and characterization methods
2. Characterization of synthetic dravite and K-dravite
3. Table: XRD and EMPA of synthetic dravite and K-dravite
4. Normalized stress vs strain plots for synthetic dravite, K-dravite, oxy-uvite, magnesio-foitite, and olenite.
5. Representative high-pressure single-crystal X-ray diffraction images and labeled diffraction spots.

1. Dravite and K-dravite synthesis and characterization

Following the procedure of Berryman et al. (2015), dravite (471-1) and K-dravite (471-2) were synthesized from their constituent oxides in the atomic proportions of the end-member species with 100% excess B and 20% excess Si (i.e., 3 MgO: 3 γ-Al_2O_3: 6 H_3BO_3: 7.2 SiO_2) in the presence of a NaCl- or KCl-saturated solution at 4.0 GPa and 700°C in an end-loaded piston-cylinder press at the GFZ German Research Centre for Geosciences with an 8-day run duration. To promote larger and more homogeneous crystal growth than achieved in Berryman et al. (2015), a chemical gradient within both synthesis experiments was created by loading each 13-mm long gold capsules first with 5.3 mg of ground SiO_2 (as quartz) and then with 9.7 mg of the ground and homogenized MgO-γ-Al_2O_3-H_3BO_3 mixture. Prior to loading either capsule with solids, ~3 μL of an NaCl- or KCl-saturated fluid was added to the dravite and K-dravite synthesis experiment, respectively. In addition to the target tourmaline species, the synthesis experiments produced coesite and pseudosinhalite as additional phases. The synthesized tourmaline was characterized by powder X-ray diffraction and electron microprobe analysis.

EMP analyses (**Table 2**) were done on the epoxy-mounted, polished, and carbon-coated samples using a JEOL Hyper- probe JXA-8500F equipped with a thermal field-emission cathode and five wavelength-dispersive spectrometers (WDS) operated with an 10.0-kV accelerating voltage, a 5-nA beam current, and a 5-µm beam diameter. Peak signals were counted for 80s (B), 40s (K), 20s (Na, Al), or 30s (Si, Mg) and background signals were counted for 40s (B), 20s (K), 10s (Na, Al), or 15s (Si, Mg). The standards used were schorl (B), orthoclase (K, Si, and Al), jadeite (Na), and periclase (Mg). Data reduction was done using a $\varphi(\rho Z)$ correction scheme (CITZAF; Armstrong 1995). Under these conditions, analytical errors (1σ) and detection limits based on counting statistics are 2.5% and 1800 ppm for B, 1% and 280 ppm for Si, 0.63% and 200 ppm for Al, 1.18% and 190 ppm for Mg, 5% and 250 ppm for Na, and 13.19% and 380 ppm for K, respectively.

For each synthesis, a finely ground portion of the solid product was glued between two boPET foils and mounted in a transmission XRD sample holder. Powder XRD patterns were recorded in the 5-125º 2θ range in 0.01º steps on a STOE Stadia P diffractometer equipped with a position-sensitive detector using $CuK_{\alpha 1}$ radiation generated with a 40-kV accelerating voltage, a 40-mA beam current, and a germanium (111) primary monochromator. Unit-cell dimensions were determined by Rietveld refinement using the GSAS software package (Larson and Von Dreele, 1987). The initial structure model applied the structural parameters of Donnay and Buerger (1950) and the average site occupancy values as determined by normalization of the EMPA.

2. Characterization of synthetic dravite and K-dravite

The unit-cell parameters determined by Rietveld refinement of the powder XRD data and the EMPA for the synthetic dravite and K-dravite are in **Table 2**. The results are normalized to either 15 cations at the Y, Z, and T sites (15 YZT) or 18 cations at the Y, Z, T, and B (18YZTB) sites, allowing for the relative amounts of O and OH at the W site to be calculated by charge balance (Henry et al., 2011). The two normalization procedures result in site occupancies that agree within error. Inclusion of the measured B in the 18 YZTB normalization results in modest amounts of B at the tetrahedral site, which is to be expected in Al-rich tourmaline synthesized at high pressure and temperature (Ertl et al., 2008a).

3. Supplementary Table. XRD and EMPA of newly synthesized tourmalines

		Dravite 471-1		**K-dravite 471-2**	
		Powder XRD	*Single-crystal XRD*	*Powder XRD*	*Single-crystal XRD*
	a_0	15.878(4) Å	15.849(2) Å	15.914(4) Å	15.904(2) Å
	c_0	7.169(2) Å	7.154(2) Å	7.164(3) Å	7.164(1) Å
	V_0	1565.3(9) Å^3	1556.4(4) Å^3	1571.4(8) Å^3	1569.2(3) Å^3
	wt.%	N = 14		N = 20	
	Na_2O	2.71(19)		0.29(16)	
	K_2O	0.02(2)		2.42(69)	
	MgO	10.4(10)		10.1(12)	
	Al_2O_3	35.1(16)		34.5(13)	
	SiO_2	34.7(16)		34.5(14)	
	B_2O_3	12.28(90)		11.13(45)	
	Total	95.2(14)		92.9(18)	
Normalization		**15 *YZT***	**18 *YZTB***	**15 *YZT***	**18 *YZTB***
X	Na	0.86(6)	0.84(6)	0.09(5)	0.09(5)
	K	0.00(0)	0.00(0)	0.51(14)	0.52(14)
	□	0.14(6)	0.16(6)	0.39(15)	0.48(14)
Y_3	Mg[a]	1.81(61)	1.77(64)	1.80(57)	1.84(55)
	Al[a]	1.19(71)	1.23(74)	1.20(62)	1.31(60)
Z_6	Mg[a]	0.72(57)	0.69(60)	0.71(50)	0.62(49)
	Al[a]	5.28(57)	5.31(60)	5.29(50)	5.38(49)
T_6	Si	5.69(22)	5.55(28)	5.73(16)	5.69(16)
	Al	0.31(22)	0.07(35)	0.27(16)	0.15(20)
	B		0.38(21)		0.17(12)
B	B	3.00[b]	3.00	3.00[b]	3.00
V_3	OH	3.00	3.00	3.00	3.00
W	OH	0.80(19)	0.77(18)	0.76(26)	0.78(9)
	O	0.12(15)	0.08(13)	0.04(6)	0.03(5)

N indicates the number of analysis spots.
[a] Mg-Al disorder between the *Y* and *Z* sites calculated using the empirical relationship of Bosi (2018)
[b] Boron content fixed to 3 atoms per formula unit in normalization

4. Supplementary Figure 1

Normalized pressure (F_E) plotted as a function of Eulerian strain (f) for each synthetic tourmaline. The symbols show the measured values and the solid and dashed lines show the 2nd and 3rd-order Birch Murnaghan PV EoS, respectively.

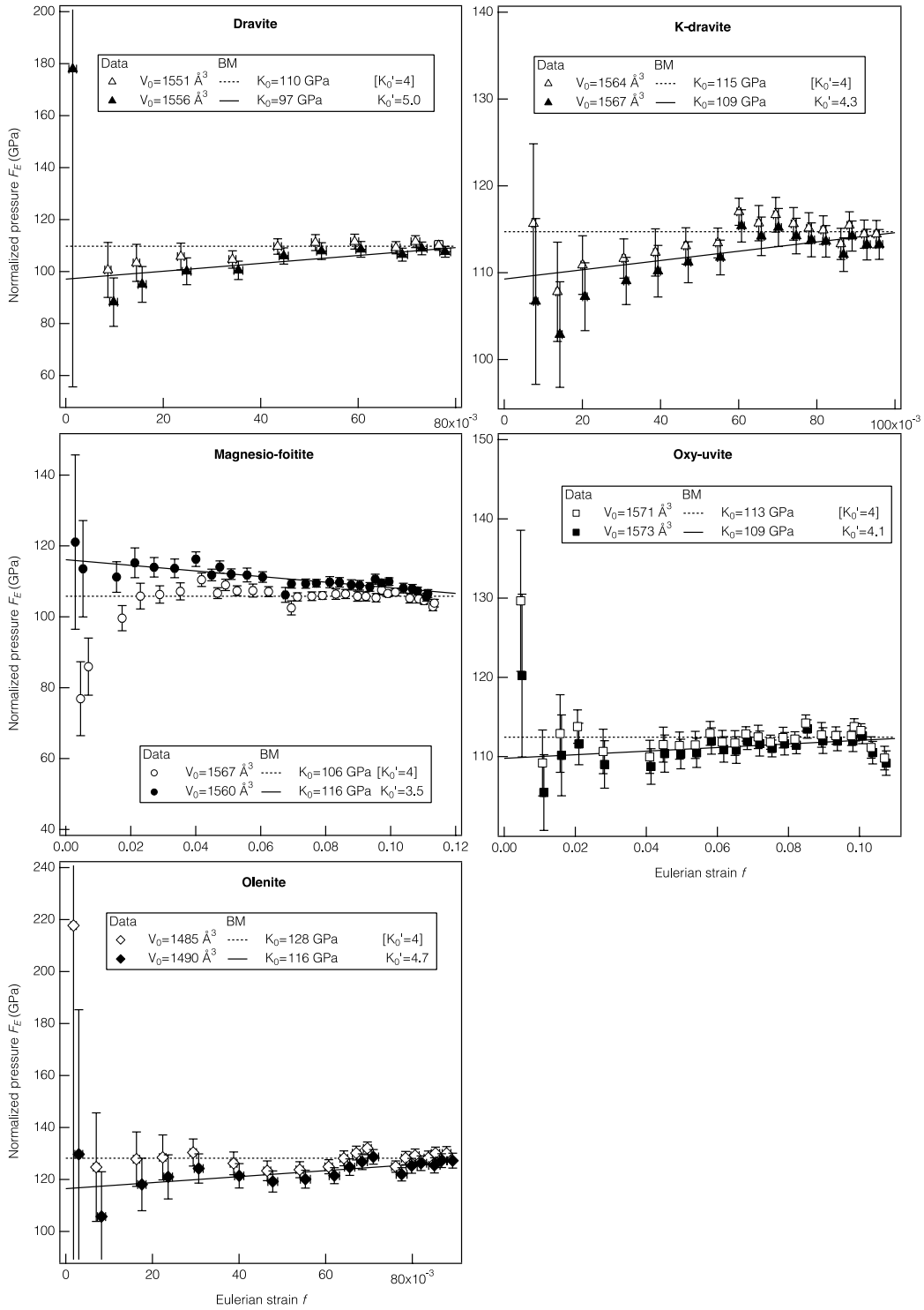

5. Supplementary Figure 2

Representative wide-scan high-pressure X-ray diffraction images for each of the synthetic tourmaline crystals. Black squares identify the peaks predicted, observed, and peak fit by the orientation matrix refined from the step-scan and wide-step scan images. The large diffraction spots are from diamond and the rings are from the rhenium gasket. The white feature is from the beam block.

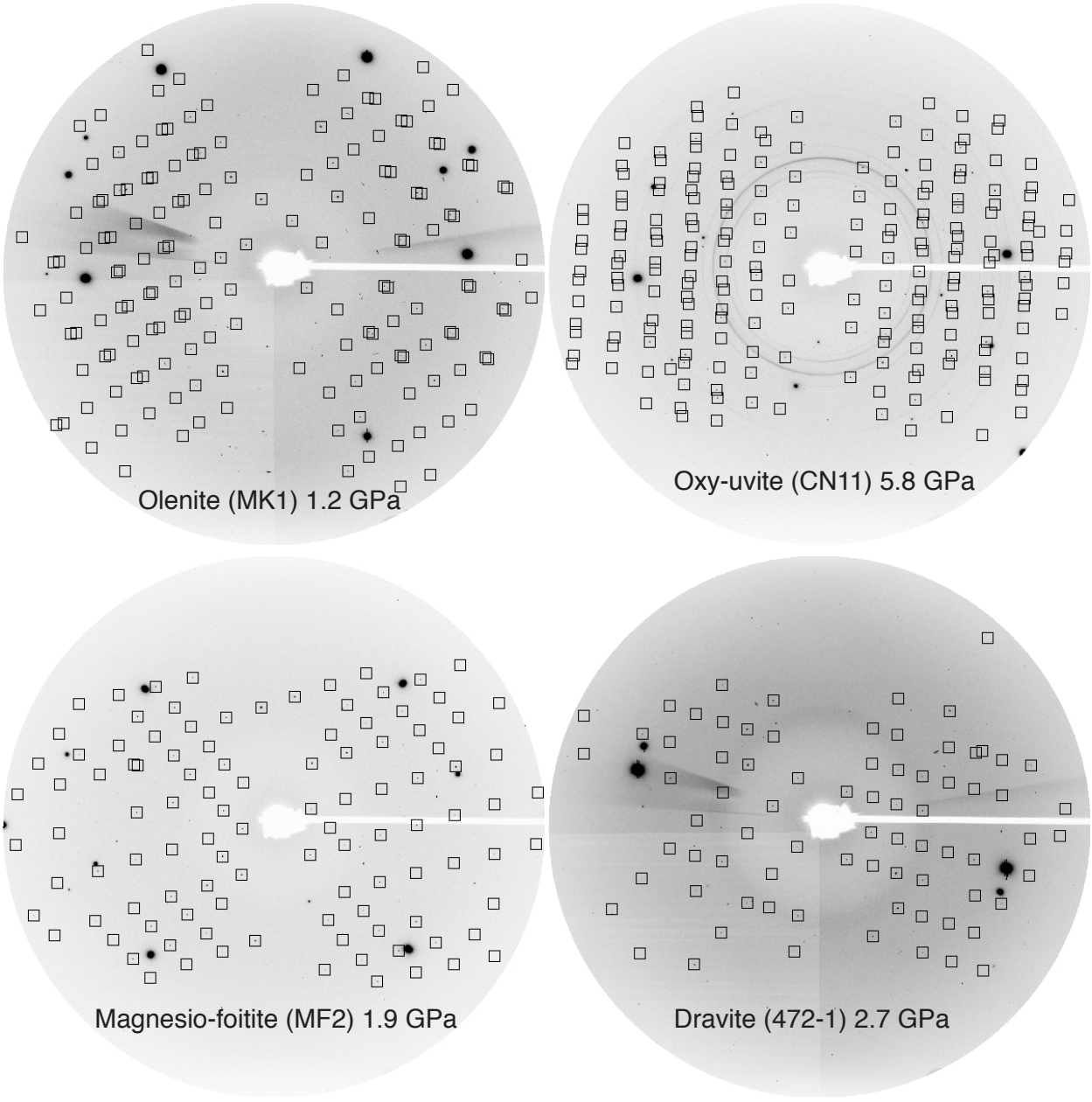

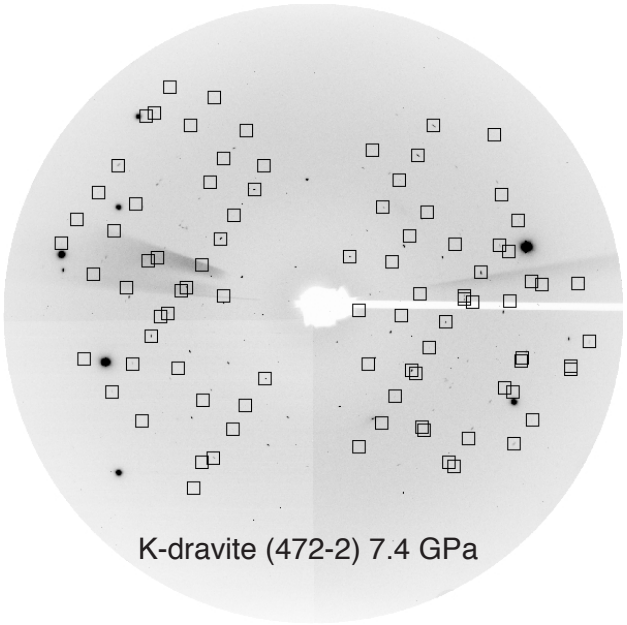
K-dravite (472-2) 7.4 GPa